Published in final edited form as:
Comput Chem Eng. 2014 November 5; 70: 180–188. doi:10.1016/j.compchemeng.2014.02.024.

Design and in silico evaluation of an intraperitoneal–subcutaneous (IP–SC) artificial pancreas

Justin J. Lee[#a,b], **Eyal Dassau**[#a,b], **Howard Zisser**[a,b], and **Francis J. Doyle III**[a,b,*]

[a]Department of Chemical Engineering, The University of California, Santa Barbara, CA 93106-5080, USA

[b]Sansum Diabetes Research Institute, 2219 Bath Street, Santa Barbara, CA 93105-4321, USA

[#] These authors contributed equally to this work.

Abstract

Prandial glucose regulation is a major challenge for the artificial pancreas using subcutaneous insulin (without a feedforward bolus) due to insulin's slow absorption-peak (50–60 min). Intraperitoneal insulin, with a fast absorption peak (20–25 min), has been suggested as an alternative to address these limitations. An artificial pancreas using intraperitoneal insulin was designed and evaluated on 100 in silico subjects and compared with two designs using subcutaneous insulin with and without a feedforward bolus, following the three meal (40–70 g-carbohydrates) evaluation protocol. The design using intraperitoneal insulin resulted in a significantly lower postprandial blood glucose peak (38 mg/dL) and longer time in the clinically accepted region (13%) compared to the design using subcutaneous insulin without a feedforward bolus and comparable results to a subcutaneous feedforward bolus design. This superior regulation with minimal user interaction may improve the quality of life for people with type 1 diabetes mellitus.

Keywords

Artificial pancreas; Insulin pump; Model predictive control; Glucose sensor; Zone model predictive control

1. Introduction

Type 1 diabetes mellitus (T1DM) is a metabolic disorder that is characterized by a lack of insulin production and secretion from the pancreatic β-cells. Since this insulin deficiency may cause people with T1DM to experience an elevated blood glucose (BG) concentration (chronic hyperglycemia, BG > 180 mg/dL) that can result in long-term damage to the eyes, nerves, and kidneys, people with T1DM are dependent on exogenous insulin to survive and to avoid diabetes complications. However, conventional exogenous insulin treatment (e.g.,

[*]Corresponding author at: Department of Chemical Engineering, The University of California, Santa Barbara, CA 93106-5080, USA. Tel.: +1 805 893 8133; fax: +1 805 893 4731. doyle@engineering.ucsb.edu..
jlee09@umail.ucsb.edu (J.J. Lee), dassau@engineering.ucsb.edu (E. Dassau), hzisser@sansum.org (H. Zisser)

multiple daily insulin injections or continuous subcutaneous insulin infusion with an insulin pump, CSII) is a cumbersome task that requires BG measurements by multiple daily finger sticks and insulin dosage estimations based on meal intake, body weight, and individual insulin-to-carbohydrates ratio. Furthermore, the insulin sensitivity of an individual (i.e., system gain) changes over time. An overdose of insulin may cause an unsafe drop in BG concentration (hypoglycemia, BG < 70 mg/dL) that if not attended can result in coma, seizure, and death. Insulin dosage estimation should be adjusted carefully and often (Lernmark, 1999; National Center for Chronic Disease Prevention and Health Promotion, 2011; Skyler, 2005; The Diabetes Control and Complications Trial Research Group, 1993).

The role of process system engineering in the biomedical field has been increasing, with one example being the effort to perform model identifications and develop control algorithms for medical applications (e.g., blood pressure control, anesthesia, and blood glucose regulation) (Bequette & Desemone, 2004; Bogle, Allen, & Sumner, 2010; Dua, Kouramas, Dua, & Pistikopoulos, 2008; Dua & Pistikopoulos, 2005; Gopinath, Bequette, Roy, Kaufman, & Yu, 1995). Specifically, an artificial pancreas (AP) that monitors glucose and delivers insulin automatically has been a topic of research since the mid 1970s, when the Biostator® became available in the hospital setting (Albisser et al., 1974; Fogi, Dodd, Jennings, & Clemens, 1978). However, the Biostator® uses intravenous (IV) glucose measurement and IV insulin delivery, and has not been evaluated for ambulatory usage due to its large size and invasive method. By contrast, SC continuous glucose monitoring (CGM) and CSII devices are smaller, less invasive, and already widely used in ambulatory diabetes care. Thus, CGM and CSII have been used in the development of an AP, and several clinical and in silico evaluations of the AP have been reported (Amrein et al., 2010; Atlas, Nimri, Miller, Grunberg, & Phillip, 2010; Breton et al., 2012; Cobelli et al., 2012; Dassau et al., 2010, 2013; Dua & Pistikopoulos, 2005; Harvey et al., 2014; Hovorka et al., 2011; Kovatchev et al., 2010; Murphy et al., 2011; Parker, Doyle, & Peppas, 1999; Patek et al., 2012; Steil, Rebrin, Darwin, Hariri, & Saad, 2006; Weinzimer et al., 2008; Zisser et al., 2012). However, substantial time delays associated with SC insulin delivery (i.e., the slow absorption peak at 50–60 min and long residence time of 6–8 h, Fig. 1) have caused a significant actuation delay of the closed-loop AP (Kovatchev, Breton, Man, & Cobelli, 2009). Consequently, postprandial hyperglycemia and late-postprandial hypoglycemia have been major challenges to a closed-loop AP without a pre-meal bolus (i.e., without manual feedforward action).

During recent decades, there has been growing industrial and academic research interest in alternative insulin administration that can deliver insulin rapidly and efficiently (see, Owens, Zinman, & Bolli, 2003; Pitt, Saudek, & Zacur, 1992; Renard, 2008). Among several delivery methods (e.g., inhaled, transdermal, oral, intradermal, etc.) that have been explored, intraperitoneal (IP) insulin delivery (i.e., insulin delivery into the abdominal cavity, Fig. 2) has received significant attention as a potential candidate for a closed-loop AP, due to its rapid pharmacokinetic characteristics (absorption peak at 20–25 min and residence time of 1–2 h) and high efficacy (Owens et al., 2003; Pitt et al., 1992; Renard, 2008; Steil, Panteleon, & Rebrin, 2004). Because of the faster absorption characteristics, an AP using IP insulin delivery has a higher closed-loop bandwidth and thus could result in better glucose regulation (e.g., faster meal disturbance rejection) compared to systems using SC insulin delivery.

In this work, an IP–SC AP that utilizes IP insulin delivery (DiaPort® 2 system from Roche Diagnostics, Basel, Switzerland) and SC CGM (Dexcom Seven® Plus from Dexcom, San Diego, U.S.) is presented, and its performance and robustness is compared with two AP designs using a conventional SC insulin delivery: SC–SC design (i.e., SC delivery and SC CGM) and the SC^{MFB}–SC design (i.e., SC–SC with manual feedforward bolus). As shown in Fig. 3, the IP–SC AP is a closed-loop design that consists of rapid acting IP insulin delivery (input/actuator), SC CGM (output/sensor), and the zone Model Predictive Control (zone-MPC) algorithm. Meal disturbance information (e.g., size and timing of a meal) is not measured or announced to the control algorithm (Table 1). Thus, the control algorithm calculates a proper dosage of insulin delivery solely based on the previous input/output history and the IP insulin delivery model that is described in the Section 3. The SC–SC AP is a closed-loop design that consists of conventional SC insulin delivery, SC CGM, and the zone-MPC algorithm with a transfer function model of SC insulin delivery that is described in the work by van Heusden, Dassau, Zisser, Seborg, and Doyle (2012). Meal disturbance information is also not measured or announced to the controller in this configuration. The SC^{MFB}–SC design consists of SC–SC design and a manual feedforward pre-meal bolus that is measured and announced by a user to the controller. Therefore, the controller adjusts its predictions and, consequently, control actions based on the pre-meal bolus amount.

Note that the IV insulin route of the UVA/Padova metabolic simulator is used as an engineering approximation for the IP insulin route in this study (Kovatchev et al., 2009), since the characteristics of the IV and the IP insulin deliveries are similar (Botz, Leibel, Zingg, Gander, & Albisser, 1976; Renard, 2008). The fast absorption and fast clearance of IV insulin compared to SC insulin is demonstrated using the UVA/Padova simulator (Kovatchev et al., 2009) in Fig. 1.

2. Methods

A 27 h clinical protocol was used to conduct in silico evaluation of the performance and robustness of the IP–SC design and compare it with the SC–SC and the SC^{MFB}–SC designs. The protocol consisted of three large unannounced meals to test disturbance rejection and a nocturnal period (24:00–8:00) to evaluate the safety of the control algorithm (e.g., no over-delivery to cause hypoglycemia while a subject is a sleep) over the period. The details of the protocol are given in the following two Sections 2.1 and 2.2. Additionally, a brief description of the zone-MPC algorithm that is utilized to calculate and deliver the optimal dosage of insulin via an insulin pump is given in Section 2.3.

2.1. In silico protocol

The closed-loop protocol started 2 h after a subject’s admission; dinner (70 g carbohydrate, g CHO), breakfast (40 g CHO), and lunch (70 g CHO) were administered at 19:00, 8:00, and 13:00, respectively (Fig. 4). In the SC^{MFB}–SC configuration, the meal size was announced to the control algorithm at the same time as the meal, and a manual SC pre-meal bolus was calculated and administered based on the individual’s insulin-to-carbohydrate ratio.

2.2. Robustness evaluation of artificial pancreas using intraperitoneal insulin delivery

For a biomedical application, the safety of the user is the first priority. Thus, any instability of the system must be avoided even with existing uncertainties in the system (e.g., inaccurate gain calculation, inter-subject variability, and circadian changes in individual insulin sensitivity). Additionally, injections of insulin into the body cannot be reversed (i.e., no negative input is allowed). Therefore, the controller must be robust against uncertainties to avoid over-delivery of insulin that may lead to an unsafe drop in BG (The Diabetes Control and Complications Trial Research Group, 1993).

The robustness of the design to 50% uncertainty in the gain was performed using the clinical protocol presented in the previous section. The value, 50%, was chosen because Boden, Chen, and Urbain, (1996) suggests that the insulin sensitivity of people with T1DM can change up to 50% during a day (i.e., lowest in the morning and highest in the evening). Additionally, a cohort of 100 in silico subjects from the UVA/Padova metabolic simulator was used to challenge the control design. The metabolic parameters of the cohort were widely spread over the parameter space to cover the significant inter-subject variability observed in medical data. The metabolic simulator has been accepted by the FDA as a pre-clinical evaluation method to ensure the safety of the controller to be tested in clinical trials (Kovatchev et al., 2009). Thus, the 50% uncertainty in the model gain combining with the 100 in silico subjects represents sufficient variability to the controller to allow robust evaluation of the design in the pre-clinical stage. Further clinical evaluation is needed to evaluate the overall robustness of the system.

2.3. Zone model predictive control

Zone-MPC is a type of model predictive control algorithm that calculates the optimal future inputs to maintain the predicted output within a desired zone rather than a single set-point. Using a zone as a control objective has several benefits. First, the controller is able to cope with sensor noise and maintain stability in the existence of model/plant mismatch better than the controller with a single set-point. However, this relaxation of the control objective may result in delayed disturbance rejection (Wang, 2002). Furthermore, in the medical context, a zone is a more suitable choice than a set-point because normoglycemia itself is defined as a zone rather than a single value (Grosman, Dassau, Zisser, Jovanovič, & Doyle, 2010; Kovatchev, Gonder-Frederick, Cox, & Clarke, 2004; Skyler, 2005). Grosman and colleagues' work demonstrated that the zone-MPC reduces control action variability compared to set-point MPC, and this ability of zone-MPC to attenuate pump activity in the presence of noisy CGM would result in a safer glucose regulation and minimal power drainage of the pump (2010).

The cost function represents the core of the zone-MPC algorithm. As given in Eq. (1), the algorithm defines the upper and lower boundaries as soft constraints that can be violated with a corresponding cost, and it calculates the optimal future input that minimizes the cost function, J_{zone}:

$$Jzone(u) = \sum_{i=1}^{P} e(k+i|k)^T Q e(k+i|k) + \sum_{j=0}^{M-1} u(k+j|k)^T R u(k+j|k),$$
$$e(k+i|k) = \begin{cases} \hat{y}(k+i|k) - y_{ub}, & \text{if } \hat{y}(k+i|k) > y_{ub} \\ 0, & \text{if } y_{lb} < \hat{y}(k+i|k) < y_{ub} \\ y_{lb} - \hat{y}(k+i|k), & \text{if } \hat{y}(k+i|k) < y_{lb} \end{cases} \quad (1)$$

where $\hat{y}(k+i|k)$, $u(k+j|k)$, y_{ub}, y_{lb}, P, M, and e are the predicted output, the predicted input, the upper boundary (140 mg/dL in this evaluation), the lower boundary (80 mg/dL in this evaluation), the prediction horizon, the control horizon, and the error, respectively. The error is defined to penalize the predicted output only when the values are outside of the zone. Therefore, when BG is within the tight range (80–140 mg/dL), the controller attenuates the high frequency sensor noise and maintains stable pump action compared to the controller with a fixed set-point (Grosman et al., 2010). In this study, the sample rate was 5 min, and the values of P and M were 8 (40 min) and 5 (25 min) time steps, respectively. The Q to R ratios used in this work were 1 to 100 and 1 to 15 for the IP–SC design and SC–SC design, respectively. The values of the P, the M, and the Q to R ratio were optimized to allow fast disturbance rejection (unannounced meal) without invoking postprandial late hypoglycemia. The Health Monitoring System (HMS) developed by Harvey and colleagues (Dassau, Jovanovič, Doyle, & Zisser, 2009; Harvey et al., 2012) was used in parallel with the zone-MPC algorithm to provide a safety system to the control layer in case that insulin modulation, control action, was insufficient in preventing hypoglycemia. The HMS automatically sends warning messages to a predetermined contact list (e.g., user, physicians, or family of the user) to take an action (consumption of 16 g CHO) when an imminent hypoglycemia is predicted.

3. Model development

For the zone-MPC algorithm to calculate the optimal dosage of insulin to regulate BG, a model that captures the dynamics between IP insulin delivery and the BG response is needed. To develop the model, a framework suggested by van Heusden and colleagues for the development of the control relevant a priori model for SC insulin delivery was utilized (van Heusden et al., 2012). As the first step in developing a model that captures the necessary dynamics, a third-order model (output error structure, with step size of 5 min) was identified for each of the ten in silico subjects from the UVA/Padova metabolic simulator (Kovatchev et al., 2009) by performing an impulse test of 1 [U] insulin bolus at steady state. Fig. 5 presents the response of the ten in silico subjects. A third-order discrete transfer function model (Eq. (2)) for each subject was identified from the impulse test by the least-squares method using the fminunc() function in MATLAB (MathWorks, Natick, MA, USA) (Ljung, 1999).

$$\frac{G(z^{-1})}{U(z^{-1})} = \frac{Kz^{-3}}{(1-p_1 z^{-1})(1-p_2 z^{-1})(1-p_3 z^{-1})} \quad (2)$$

K, p_1, p_2, p_3 are the gain (the values of the ten subjects are between 3×10^{-2} and 3×10^{-1}, when the units for the input and output are U/h and mg/dL, respectively), the first pole, the second pole, and the third pole of the model, respectively. The coefficient of determination,

R^2, values of the models were between 0.72 and 0.84, and the locations of the poles of the identified models are given in Table 2. A higher-order model did not achieve a significantly better value for the coefficient of determination.

Since the systems do not have a resonant frequency (or a resonant peak), a model that captures the dynamics around the estimated closed-loop bandwidth is sufficient for the robustness of the controller (van Heusden et al., 2012). The poles of the models in Table 2 strongly suggest that a dominant structure is the third order model with one slower pole (i.e., the value between 0.97 and 0.99) and two faster poles (i.e., the value between 0.68 and 0.76). Based on this observation, a control relevant model, M_r, for IP insulin delivery is proposed as follows:

$$M_r\left(z^{-1}\right)=\frac{G\left(z^{-1}\right)}{U\left(z^{-1}\right)}=\frac{K_m z^{-3}}{\left(1-0.98z^{-1}\right)\left(1-0.75z^{-1}\right)^2}, \quad (3)$$

$K_m = 2.5 \times 10^{-1}$, when the units for the input and output are U/h and mg/dL, respectively.

The robustness of the control algorithm, based on the proposed model, was analyzed. As the first step, the closed-loop bandwidth of a set-point MPC using the proposed model was estimated by measuring the rise time of a set-point change for each subject. The inverse relationship between the rise time and the closed-loop bandwidth was utilized in the estimation as suggested by Astrom and Murray (Astrom & Murray, 2008; Maciejowski, 1989). The estimated closed-loop bandwidths of each of the ten runs (i.e., the controller and the ten subjects) are listed in Table 3. At the region of the estimated closed-loop bandwidth in the bode diagram (the gray shaded region between 1.2×10^{-2} rad/min and 8.0×10^{-2} rad/min in Fig. 6), the phase angle of the proposed control relevant model is lower than that of the ten identified individual models, and the gain of the proposed model is overestimated. Thus, the controller based on the proposed model may be more robust than the one based on the individual models (Maciejowski, 1989; van Heusden et al., 2012). The frequency analysis also shows that the estimated closed-loop bandwidth of the IP–SC design (between 1.2×10^{-2} rad/min and 8.0×10^{-2} rad/min, or the rise time between 25 min and 160 min) is considerably larger than that of the SC–SC design (between 6.0×10^{-3} rad/min and 3.6 10^{-3} rad/min, or the rise time between 330 min and 550 min) (van Heusden et al., 2012). Hence, the IP–SC design with the larger closed-loop bandwidth may reject a disturbance and achieve a control objective significantly faster than the SC–SC design. Subsequently, the IP–SC design would provide better glucose regulation with faster disturbance rejection and less overshoot.

In order to account for inter-subject variability, the gain of the model is personalized by using a correction factor (Davidson, Hebblewhite, Steed, & Bode, 2009). The personalized model, M_i, is given below:

$$M_i\left(z^{-1}\right)=\frac{G\left(z^{-1}\right)}{U\left(z^{-1}\right)}=\frac{F_s K_i c z^{-3}}{\left(1-0.98z^{-1}\right)\left(1-0.75z^{-1}\right)^2}, \quad (4)$$

where F_s, K_i, and c are the safety factor (1.5 for this study), the individual gain based on the 2400 rule (Walsh, 2009), and the conversion factor c (6.25×10^{-3} for the input and output are U/h and mg/dL), respectively. K_i is defined by the following equation:

$$K_i = \frac{2400}{TDI}. \quad (5)$$

If the individual gain K_i were to be under- or overestimated, the safety factor F_s could be adjusted to compensate for the mismatch (van Heusden et al., 2012). This individualized model is incorporated into the zone-MPC algorithm in this study.

4. Results

The performance evaluation of the IP–SC AP and comparison with SC–SC AP and SC^{MFB}–SC AP are presented in Section 4.1. The average population summary of 100 in silico subjects and a control action comparison of a representative individual case are shown below. The robustness evaluation of the IP–SC AP that represents the worst case of 50% uncertainty in the model gain that are results of erroneous TDI calculation and intra-subject insulin sensitivity variation is presented in Section 4.2.

4.1. In silico evaluation of the IP–SC design

The average BG profiles during the in silico evaluation (Fig. 7) illustrate that the average postprandial BG peak was lower by 38 mg/dL in the IP–SC case than the SC–SC case. Also, after the meal, the IP–SC design brought average BG back into the clinically accepted region (70–180 mg/dL) significantly faster by 1.5–2 h than the SC–SC design (Fig. 7 and Table 4, the p-value < 0.01 for the paired t-test). The average percentages of time in Table 4, $t_{average}$, were calculated as the following equation:

$$t_{\text{average}} = \frac{\sum_{k=1}^{n} t_{\text{individual}}}{n} \quad (6)$$

where $t_{individual}$ and n are the individual's percentage of time in a desired zone during a period and the number of subjects, 100. Furthermore, control variability grid analysis (CVGA, Fig. 8) was also done to compare the quality of the closed-loop control. The CVGA is a widely accepted performance index that reflects the quality of the closed-loop glucose regulation on a cohort of subjects by emphasizing the extreme values (i.e., minimum and maximum). The CVGA classifies the control quality into nine categories, which are represented as nine rectangular zones on the plane as follows: A zone (accurate control), three B zones (benign deviations from accurate control), two C zones (over-corrections of hyper-/hypoglycemia), two D zones (failure to deal with hyper-/hypoglycemia), and one E zone (erroneous control). The points closer to the origin (i.e., the A zone) represent the most effective control (Magni et al., 2008). The analysis demonstrated that the IP–SC design resulted in better BG regulation (17% in the A zone, 83% in the B zone) than the SC–SC design (4% in the A zone, 86% in the B zone, and 4% in the C, and 6% in the D zone). Additionally, a quantitative way to project the different performances of the three designs is

the use of the BG risk indices, the High Blood Glucose Index (HBGI) and the Low Blood Glucose Index (LBGI). These indices demonstrate the relative risk of either low or high BG, and yield a value between 0 and 100 (a higher number corresponds to a higher risk). This method is described in Kovatchev and colleagues' work, and a brief description of the calculation is given below (Kovatchev, Cox, Gonder-Frederick, & Clarke, 1997; Kovatchev et al., 1998).

First, the BG measurement readings were transformed into a symmetric scale using the following equation:

$$BG^{*}=1.509\cdot\left(\left[log\left(BG\right)\right]^{1.084}-5.381\right). \quad (7)$$

The BG risk function, *R*, was defined as:

$$R\left(BG\right)=10\cdot BG^{*2} \quad (8)$$

The low BG risk, LR, was then determined by the following equation:

$$LR\left(BG\right)=R\left(BG\right), \quad \text{if } BG<112.5\,mg/dL, \text{ and } 0 \text{ otherwise}, \quad (9)$$

and the high BG risk, HR, was calculated by the following equation:

$$HR\left(BG\right)=R\left(BG\right), \quad \text{if} \quad BG>112.5\,mg/dL, \text{ and } 0 \text{ otherwise}. \quad (10)$$

Since there were multiple BG readings, the LBGI and HBGI were calculated as the average of the multiple LR and HR values, respectively (Kovatchev et al., 1997, 1998). The BG risk indices calculation (Table 5) showed that the IP–SC design is a superior glucose regulation scheme compared to the SC–SC design (HBGI were 2.74 and 1.53 in SC–SC and IP–SC cases, respectively).

When compared against the SC^{MFB}–SC design that includes manual meal boluses, the IP–SC design achieved comparable BG regulation without user interaction (i.e., no manual feedforward control action). Total time spent in the clinically accepted region (Table 4) was not significantly different (i.e., 1% difference) in the SC^{MFB}–SC case and the IP–SC case, and the two BG standard deviation envelopes (Fig. 7) had considerable overlaps between each other. The postprandial BG peak was 22 mg/dL lower in the SC^{MFB}–SC case than the IP–SC case (Fig. 7), and the HBGI of the SC^{MFB}–SC case, 1.10, was slightly lower than the value of the IP–SC case, 1.53 (Table 5). However, the lower BG peak and smaller HBGI were achieved by using the perfect information (i.e., accurate estimation of the meal size and individual insulin-to-carbohydrate ratio) and user interaction. In real-world situation, the meal size and individual insulin-to-carbohydrate ratio always contain uncertainty, and the uncertainty may cause problem for the SC^{MFB}–SC design (e.g., hypoglycemia from insulin overdose). Furthermore, CVGA (Fig. 8) demonstrated that the IP–SC design resulted in equivalent BG regulation (100% in the A + B zone, 0% in the C zone, and 0% in the D zone) compared to the SC^{MFB}–SC design (97% in the A + B zone, 1% in C zone, and 2% in D zone).

To illustrate the differences between the control actions of three controller configurations, the individual controller action profiles along with the CGM traces of all cases are presented in Fig. 9. As can be seen, the three designs were able to reject this disturbance but with significant time differences (i.e., 3 h, 1.4 h, and 1.2 h before the output, BG, came back to the clinically accepted region for the SC–SC, and IP–SC, and the SC^{MFB}–SC designs, respectively). As noted, the actuation delay (transport delay of SC insulin) in the SC–SC design resulted in slow disturbance rejection because an unannounced meal disturbance was a significant challenge to the control system, due to the fast effect of a meal on glucose (~15–20 min). On the other hand, the IP–SC design was able to respond to the unannounced meal disturbance quicker and bring BG back into the clinically accepted region less than 2 h in each post-prandial period. In addition to this faster disturbance rejection, the IP–SC design achieved a 20 mg/dL (ranging from 10 to 26 mg/dL) lower mean postprandial peak compared to the SC–SC design. Furthermore, due to minimal transport delay of IP insulin (insulin peak at 20–30 min and 50–60 min for IP insulin and SC insulin, respectively), the IP–SC design was able to take more aggressive action than SC–SC design during the postprandial periods (i.e., the IP–SC design delivered larger amount of insulin at the beginning of the period, Fig. 9), and this aggressive action resulted in a faster disturbance rejection without causing an overshoot (i.e., hypoglycemia).

Comparing the SC^{MFB}–SC design and the IP–SC design, the SC^{MFB}–SC design resulted in 4% longer time in the target region and 21 mg/dL (ranging from 8 to 32 mg/dL) lower mean postprandial peak. However, the SC^{MFB}–SC design used noticeably more insulin than the IP–SC design to achieve a similar effect. During the post-prandial periods, mean insulin usage were 152% above the basal (ranging from 101% to 183%) and 85% above the basal (ranging from 60% to 105%) in the SC^{MFB}–SC (including the pre-meal bolus) and the IP–SC cases, respectively. The SC^{MFB}–SC design utilized more insulin, and, furthermore, the design required the accurate insulin-to-carbohydrate ratio of the individual.

4.2. Robustness evaluation of IP–SC design

The results of the robustness evaluation (Tables 6 and 7) showed that the controller could safely operate even with various uncertainties. The average time in the clinically accepted region (Table 6) decreased only by 5% and 9% in the 50% under- and overestimated model gain cases, respectively, compared to the nominal case, and this showed that the controller's performance would not be significantly deteriorated by the uncertainty from the insulin sensitivity's circadian change or TDI miscalculation. Furthermore, no instability of the system (e.g., divergence or oscillation of BG) was observed during the evaluation using the 100 in silico subjects, and this indicated that the controller can perform properly even with existence of a large inter-subject variability. Most importantly, no severe hypoglycemia (BG < 50 mg/dL, Table 7) was observed. A few subjects experienced mild hypoglycemia (50 mg/dL < BG < 70 mg/dL), but the average duration of the mild hypoglycemia was short for all cases (i.e., approximately 35 min). Additionally, the number of hypoglycemia treatments given by the HMS for all three cases were not significantly different from one to another (i.e., the difference in the total number of the treatments was less than 5), and this showed that 50% uncertainty in the gain would not result in unsafe over-delivery of insulin. None of the subjects experienced multiple hypoglycemic episodes during the evaluation, except for a

single isolated event. Also, the average low BG index of the subjects who experienced hypoglycemia was low: 0.42, 0.35, and 0.31 in the underestimated, the nominal, and the overestimated model gain cases, respectively, all of which fall well below the low-hypoglycemia-risk threshold of 2.5 (Kovatchev et al., 1998).

5. Discussion

Subcutaneous insulin delivery has been the basis of insulin therapy for people with T1DM since 1922. Although the SC delivery is minimally invasive and user-friendly, it exhibits inherent slow absorption characteristics as well as the risk of insulin depot in the SC space (i.e., insulin remains in the SC region instead of diffusing into the blood vessels) (Schaepelynck et al., 2011). In the development of a closed-loop AP, the insulin depot effect and slow absorption characteristics limits the controller's ability to achieve normoglycemia and introduces hypoglycemia risk.

Hence, the fast-absorbing IP route that delivers insulin into the abdominal cavity may provide a breakthrough method in an AP development. Since IP insulin is absorbed by the capillary bed in the region (portal venous system), there is a significantly less transport delay or insulin depot effect (Pitt et al., 1992; Schaepelynck et al., 2011). The closed-loop AP using the IP route with the advantages mentioned above may result in better meal disturbance rejection without presenting a hypoglycemia risk, as shown in Section 4 (i.e., the IP–SC design resulted in 20% longer time in the clinically accepted region than the SC–SC design without inducing extra hypoglycemia events). Even though the IP insulin delivery has its own minimal risks associated with the surgical procedure, it may be a promising strategy for insulin treatments and the AP development. Additionally, due to the fast absorption characteristics, regular human insulin can be used in the insulin therapy instead of insulin analogs (i.e., modified form of insulin that has a faster absorption characteristic), and this may reduce the financial burden of the insulin treatments for the people with T1DM in the long run.

As shown in Section 4, a meal announcement to the controller (i.e., manual feedforward SC bolus in the SC^{MFB}–SC design) can significantly improve the performance of the controller at meal time (i.e., 21% increase of time in the clinically accepted region compared to the SC–SC design), but the bolus estimation brings possible human errors into the system. In real-world situations, inaccurate calculation of the bolus size or missing meal bolus injection happen frequently, and the erroneous meal announcement when using the AP may result in an unsafe BG decline or prolonged high BG period after a meal. Thus, the IP–SC design that required no user-interaction, yet achieved comparable BG regulation as shown in Section 4 (i.e., 1% difference of time in the clinically accepted region), would be considered as a superior BG treatment option to the SC^{MFB}–SC design. However, an experienced user who wants an additional degree of control may prefer SC^{MFB}–SC design.

Even though the possible benefit of pre-meal IP bolus was conceivable, IP–SC design with manual feedforward IP bolus was not considered in this work because of the possibility of the safety hazard from an inaccurate bolus calculation mentioned above. Additionally, because of the rapid absorption rate of IP insulin, the risk of overestimated IP bolus or

delayed meal intake would be even bigger than the risk of SC case. This safety risk would nullify the possible benefit of pre-meal IP bolus. Furthermore, the time window for providing the standard hypoglycemia treatment (e.g., glucose tablet or fruit juice) to reverse the overdose might be too short.

6. Conclusions

The in silico evaluation showed that the IP–SC design achieved superior glucose regulation over the SC–SC design. The IP–SC design rejected the meal disturbances significantly faster than the SC–SC design without additional overshoot (late postprandial hypoglycemia). During the postprandial periods, the IP–SC design brought the output back into the desired zone faster by 1.5–2 h and achieved a 38 mg/dL lower peak on average compared to the SC–SC design. The evaluation also showed that the IP–SC design without user interactions achieved similar BG regulation compared to the SC^{MFB}–SC design that requires manual meal bolus injections. Hence, the fast action and rapid clearance of IP insulin reduced the burden of the user to maintain BG within the clinically accepted region by eliminating the actuation delay of the closed-loop system. Furthermore, the robustness evaluation suggested that the IP–SC design could operate safely with 50% uncertainty in the model gain. Enhanced glycemic control with the IP–SC design could reduce the effect of meal disturbance (hyperglycemia and hypoglycemia) and improve the quality of life of people with the disorder.

Acknowledgments

Funding sources This work was funded by the JDRF, grant #: 17-2011-515 and the National Institutes of Health, grant #: DP3-DK094331 and R01-DK085628

Abbreviations

T1DM	type 1 diabetes mellitus
BG	blood glucose
CSII	continuous subcutaneous insulin infusion
AP	artificial pancreas
IP	intraperitoneal
IV	intravenous
SC	subcutaneous
CGM	continuous glucose monitor
MPC	model predictive control
PK	pharmacokinetics
PD	pharmacodynamics
CHO	carbohydrate
HBGI	high blood glucose index

LBGI	low blood glucose index
CVGA	control variability grid analysis

References

Albisser AM, Leibel BS, Ewart TG, Davidovac T, Botz CK, Zingg W. An artificial endocrine pancreas. Diabetes. 1974; 23:389–396. [PubMed: 4598089]

Amrein K, Ellmerer M, Hovorka R, Kachel N, Parcz D, Korsatko S, et al. Hospital glucose control: Safe and reliable glycemic control using enhanced model predictive control algorithm in medical intensive care unit patients. Diabetes Technology & Therapeutics. 2010; 12:405–412. [PubMed: 20388051]

Astrom, KJ.; Murray, RM. Feedback systems: An introduction for scientist and engineers. Princeton University Press; Princeton. NJ: 2008.

Atlas E, Nimri R, Miller S, Grunberg EA, Phillip M. MD-logic artificial pancreas system: A pilot study in adults with Type 1 diabetes. Diabetes Care. 2010; 33:1072–1076. [PubMed: 20150292]

Bequette BW, Desemone J. Intelligent dosing system: Need for design and analysis based on control theory. Diabetes Technology & Therapeutics. 2004; 6:868–873. [PubMed: 15684641]

Boden G, Chen X, Urbain JL. Evidence for a circadian rhythm of insulin sensitivity in patients with NIDDM caused by cyclic changes in hepatic glucose production. Diabetes. 1996; 45:1044–1050. [PubMed: 8690150]

Bogle IDL, Allen R, Sumner T. The role of computer aided process engineering in physiology and clinical medicine. Computers & Chemical Engineering. 2010; 34:763–769.

Botz CK, Leibel BS, Zingg W, Gander RE, Albisser AM. Comparison of peripheral and portal routes of insulin infusion by a computer-controlled insulin infusion system (artificial endocrine pancreas). Diabetes. 1976; 25:691–700. [PubMed: 782981]

Breton M, Farret A, Bruttomesso D, Anderson S, Magni L, Patek S, et al. Fully integrated artificial pancreas in Type 1 diabetes: Modular closed-loop glucose control maintains near normoglycemia. Diabetes. 2012; 61:2030–2037. [PubMed: 22596052]

Cobelli C, Renard E, Kovatchev BP, Keith-Hynes P, Ben Brahim N, Place J, et al. Pilot studies of wearable outpatient artificial pancreas in Type 1 diabetes. Diabetes Care. 2012; 35:e65–e67. [PubMed: 22923687]

Dassau E, Jovanovič L, Doyle FJ III, Zisser H. Enhanced 911/GPS wizard: A telemedicine application for the prevention of severe hypoglycemia – monitor, alert and locate. Journal of Diabetes Science and Technology. 2009; 3:1501–1506. [PubMed: 20144406]

Dassau E, Zisser H, Percival MW, Grosman B, Jovanovič L, Doyle FJ III. Clinical results of automated artificial pancreatic β-cell system with unannounced meal using multi-parametric MPC and insulin-on-board. Diabetes. 2010; 59(1):A94.

Dassau E, Zisser H, Harvey RA, Percival MW, Grosman B, Bevier W, et al. Clinical evaluation of a personalized artificial pancreas. Diabetes Care. 2013; 36:801–809. [PubMed: 23193210]

Davidson PC, Hebblewhite HR, Steed RD, Bode BW. Analysis of guidelines for basal-bolus insulin dosing: Basal insulin, correction factor, and carbohydrate-to-insulin ratio. Endocrine Practice. 2009; 14:1095–1101. [PubMed: 19158048]

Dua P, Pistikopoulos EN. Modelling and control of drug delivery systems. Computers & Chemical Engineering. 2005; 29:2290–2296.

Dua P, Kouramas K, Dua V, Pistikopoulos EN. MPC on a chip – Recent advances on the application of multi-parametric model-based control. Computers & Chemical Engineering. 2008; 32:754–765.

Fogi E, Dodd L, Jennings E, Clemens A. Development and evaluation of a glucose analyzer for a glucose-controlled insulin infusion system (Biostator). Clinical Chemistry. 1978; 24:1366–1372. [PubMed: 679460]

Gopinath R, Bequette BW, Roy RJ, Kaufman H, Yu C. Issues in the design of a multirate model-based controller for a nonlinear drug infusion system. Biotechnology Progress. 1995; 11:318–332. [PubMed: 7619401]

Grosman B, Dassau E, Zisser H, Jovanovič L, Doyle FJ III. Zone model predictive control: a strategy to minimize hyper- and hypoglycemic events. Journal of Diabetes Science and Technology. 2010; 4:961–975. [PubMed: 20663463]

Harvey RA, Dassau E, Zisser H, Seborg DE, Jovanovič L, Doyle FJ III. Design of the health monitoring system for the artificial pancreas: Low glucose prediction module. Journal of Diabetes Science and Technology. 2012; 6:1345–1354. [PubMed: 23294779]

Harvey RA, Dassau E, Bevier W, Seborg DE, Jovanovič L, Doyle FJ III, et al. Clinical evaluation of an automated artificial pancreas using zone-model predictive control and health monitoring system. Diabetes Technology & Therapeutics. 2014 [Epub ahead print].

Hovorka R, Kumareswaran K, Harris J, Allen JM, Elleri D, Xing D, et al. Overnight closed loop insulin delivery (artificial pancreas) in adults with Type 1 diabetes: crossover randomised controlled studies. British Medical Journal. 2011; 342:d1855. [PubMed: 21493665]

Kovatchev BP, Cox DJ, Gonder-Frederick LA, Clarke W. Symmetrization of the blood glucose measurement scale and its applications. Diabetes Care. 1997; 20:1655–1658. [PubMed: 9353603]

Kovatchev BP, Cox DJ, Gonder-Frederick LA, Young-Hyman D, Schlundt D, Clarke W. Assessment of risk for severe hypoglycemia among adults with IDDM: Validation of the low blood glucose index. Diabetes Care. 1998; 21:1870–1875. [PubMed: 9802735]

Kovatchev BP, Gonder-Frederick LA, Cox DJ, Clarke WL. Evaluating the accuracy of continuous glucose-monitoring sensors: Continuous glucose-error grid analysis illustrated by therasense freestyle navigator data. Diabetes Care. 2004; 27:1922–1928. [PubMed: 15277418]

Kovatchev BP, Breton M, Man CD, Cobelli C. In silico preclinical trials: A proof of concept in closed-loop control of Type 1 diabetes. Journal of Diabetes Science and Technology. 2009; 3:44–55. [PubMed: 19444330]

Kovatchev BP, Cobelli C, Renard E, Anderson S, Breton M, Patek S, et al. Multinational study of subcutaneous model-predictive closed-loop control in Type 1 diabetes mellitus: summary of the results. Journal of Diabetes Science and Technology. 2010; 4:1374–1381. [PubMed: 21129332]

Lernmark A. Type 1 diabetes. Clinical Chemistry. 1999; 45:1331–1338. [PubMed: 10430815]

Ljung, L. System identification theory for the user. 2nd ed. Prentice Hall; Upper Saddle River, NJ: 1999.

Maciejowski, JM. Multivariable feedback design. Addison Wesley; Great Britain: 1989.

Magni L, Raimondo DM, Dalla Man C, Breton M, Patek S, De Nicolao G, et al. Evaluating the efficacy of closed-loop glucose regulation via control-variability grid analysis. Journal of Diabetes Science and Technology. 2008; 2:630–635. [PubMed: 19885239]

Murphy HR, Kumareswaran K, Elleri D, Allen JM, Caldwell K, Biagioni M, et al. Safety and efficacy of 24-h closed-loop insulin delivery in well-controlled pregnant women with Type 1 diabetes: A randomized crossover case series. Diabetes Care. 2011; 34:2527–2529. [PubMed: 22011408]

National Center for Chronic Disease Prevention and Health Promotion. [Accessed 22.07.13] National Diabetes Fact Sheet. National Center for Chronic Disease Prevention and Health Promotion. 2011. http://www.cdc.gov/diabetes/pubs/pdf/ndfs_2011.pdf

Owens DR, Zinman B, Bolli G. Alternative routes of insulin delivery. Diabetic Medicine. 2003; 20:886–898. [PubMed: 14632713]

Parker RS, Doyle FJ III, Peppas NA. A model-based algorithm for blood glucose control in Type 1 diabetic patients. IEEE Transactions on Biomedical Engineering. 1999; 46:148–157. [PubMed: 9932336]

Patek SD, Magni L, Dassau E, Karvetski C, Toffanin C, De Nicolao G, et al. Modular closed-loop control of diabetes. IEEE Transactions on Biomedical Engineering. 2012; 59:2986–2999. [PubMed: 22481809]

Pitt HA, Saudek CD, Zacur HA. Long-term intraperitoneal insulin delivery. Annals of Surgery. 1992; 216:483–491. [PubMed: 1417197]

Renard E. Insulin delivery route for the artificial pancreas: subcutaneous, intraperitoneal, or intravenous? Pros and Cons. Journal of Diabetes Science and Technology. 2008; 2:735–738. [PubMed: 19885254]

Schaepelynck P, Renard E, Jeandidier N, Hanaire H, Fermon C, Rudoni S, et al. A recent survey confirms the efficacy and the safety of implanted insulin pumps during long-term use in poorly controlled Type 1 diabetes patients. Diabetes Technology & Therapeutics. 2011; 13:657–660. [PubMed: 21470000]

Skyler, JS. Atlas of diabetes. 3rd ed. Current Medicine Group LLC; Philadelphia, PA: 2005.

Steil GM, Panteleon AE, Rebrin K. Closed-loop insulin delivery-the path to physiological glucose control. Advanced Drug Delivery Reviews. 2004; 56:125–144. [PubMed: 14741112]

Steil GM, Rebrin K, Darwin C, Hariri F, Saad MF. Feasibility of automating insulin delivery for the treatment of Type 1 diabetes. Diabetes. 2006; 55:3344–3350. [PubMed: 17130478]

The Diabetes Control and Complications Trial Research Group. The effect of intensive treatment of diabetes on the development and progression of long-term complications in insulin-dependent diabetes mellitus. New England Journal of Medicine. 1993; 329:977–986. [PubMed: 8366922]

van Heusden K, Dassau E, Zisser H, Seborg DE, Doyle FJ III. Control-relevant models for glucose control using a priori patient characteristics. IEEE Transactions on Biomedical Engineering. 2012; 59:1839–1849. [PubMed: 22127988]

Walsh, J. [Accessed 22.07.13] Preliminary Proposal For Insulin Pump Standard. Diabetes Services. 2009. http://www.diabetesnet.com/diabetespresentations/PropInsPumpManufStand-0909.html

Wang, Y. Robust Model Predictive Control (Ph.D. dissertation). University of Wisconsin-Madison; Madison, WI: 2002.

Weinzimer SA, Steil GM, Swan KL, Dziura J, Kurtz N, Tamborlane WV. Fully automated closed-loop insulin delivery versus semiautomated hybrid control in pediatric patients with Type 1 diabetes using an artificial pancreas. Diabetes Care. 2008; 31:934–939. [PubMed: 18252903]

Zisser H, Dassau E, Harvey RA, Bevier W, Jovanovič L, Doyle FJ III. Clinical evaluation of a fully automated artificial pancreas using zone-model predictive control with health monitoring system. Diabetes. 2012; 61(1A):LB8.

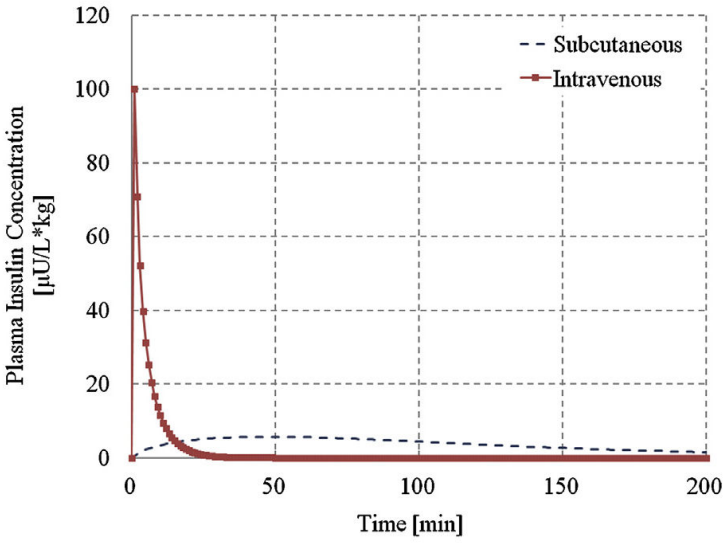

Fig. 1.

Comparison between subcutaneous and intravenous absorption rates of a subject from the UVA/Padova metabolic simulator (Kovatchev et al., 2009) following a delivery of one insulin unit.

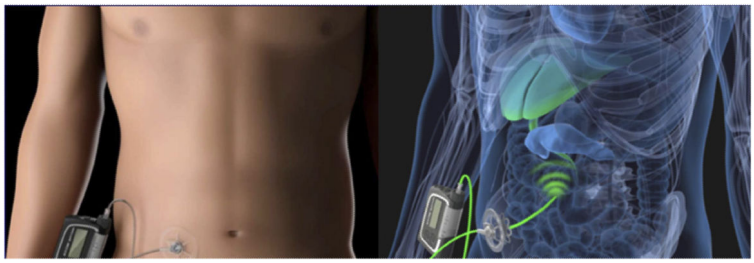

Fig. 2.

Schematic depiction of DiaPort® 2 system. (Left panel) An Accu-Chek® insulin pump that contains and delivers insulin via the DiaPort® 2 injection site on the abdomen region. The injection site consists of a plastic cannula, a metal port, and a plastic tube. (Right panel) Animated description of insulin delivery to the intraperitoneal cavity. Insulin from the pump flows through the tube and disperse into the abdominal cavity (courtesy of Roche Corporation).

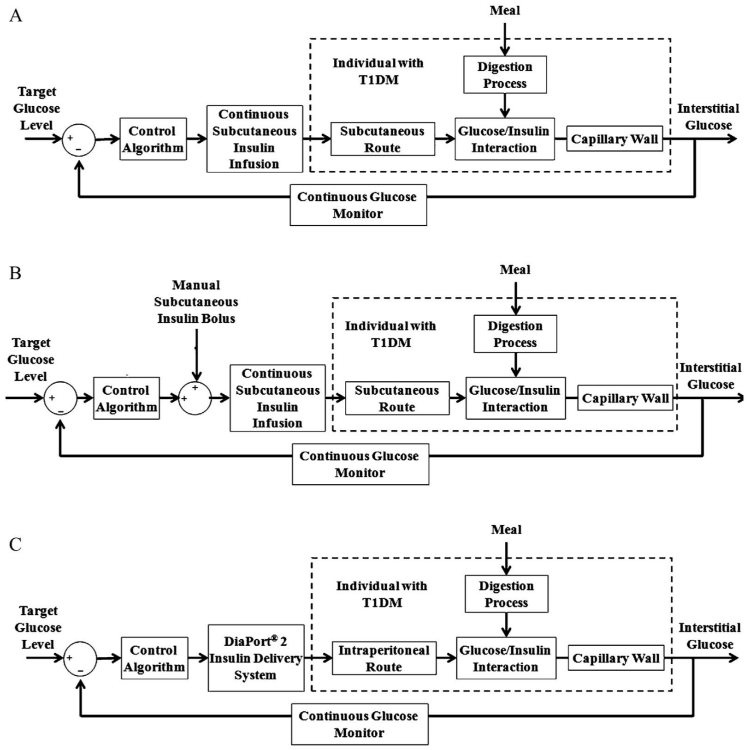

Fig. 3.

Block diagrams of the three artificial pancreas configurations: (A) closed-loop system using the subcutaneous route (i.e., SC–SC design), (B) SC–SC design with manual feedforward bolus (i.e., SC^{MFB}–SC design), and (C) closed-loop system using the intraperitoneal route (i.e., IP–SC design).

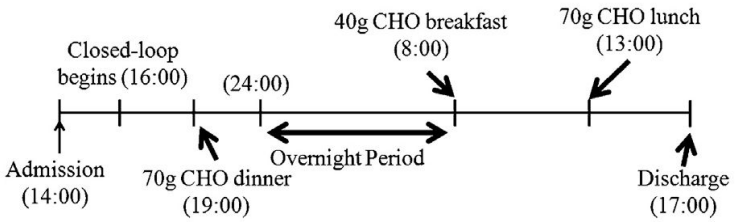

Fig. 4.

Descriptive time line of the in silico protocol that was adopted from the clinical protocol.

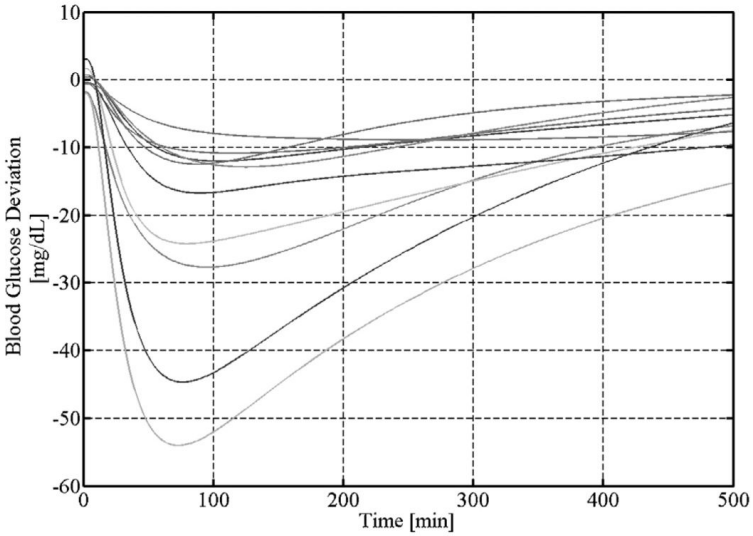

Fig. 5.

Blood glucose deviation of the ten in silico subjects after an injection of 1 U insulin through the intravenous port of the UVA/Padova FDA-accepted metabolic simulator (Kovatchev et al., 2009).

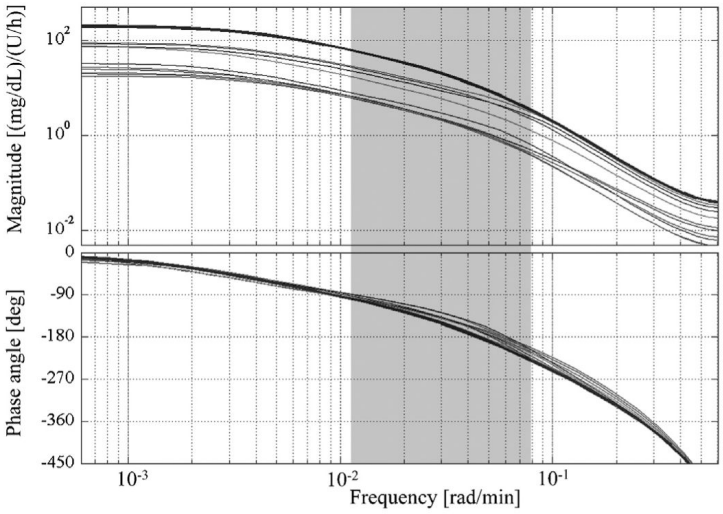

Fig. 6.

Bode diagram of the ten identified models of the in silico subjects (thin gray lines) and the proposed control relevant model (black bold line). The gray shaded region represents the frequency band around the estimated closed-loop bandwidth.

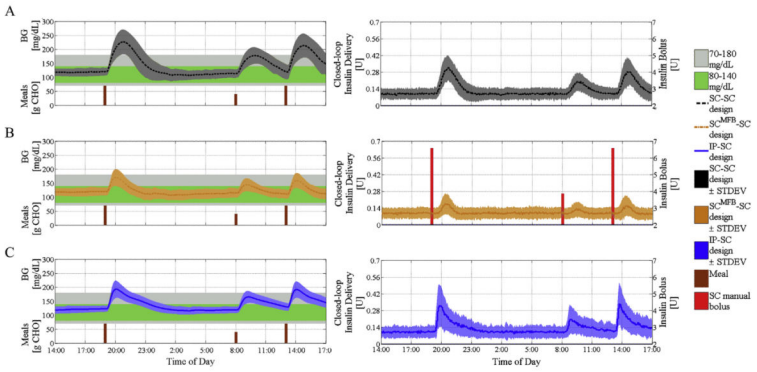

Fig. 7.

Summary of the three controller configurations for one hundred in silico subjects, Left panels: Average blood glucose ± STDEV in the SC–SC design (A, black dashed line and shaded region), the SC^{MFB}–SC design (B, orange dashed-dot line and shaded region), and the IP–SC design (C, blue solid line and shaded region) cases. Also, the meal sizes (brown bars) are indicated, Right panels: Average insulin delivered via an insulin pump ± STDEV in the SC–SC design (A), the SC^{MFB}–SC design (B), and the IP–SC design (C) cases. Manual insulin bolus sizes (red bars) are on the right *y*-axis. (For interpretation of the references to color in this figure legend, the reader is referred to the web version of the article.)

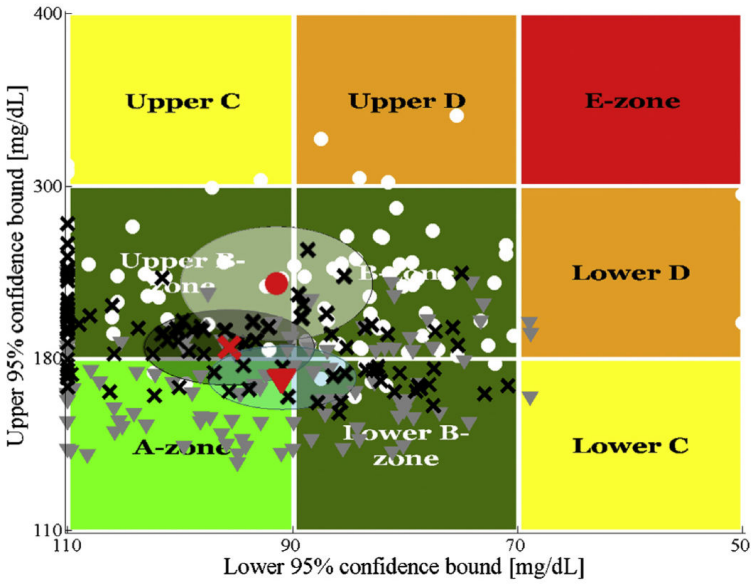

Fig. 8.

Evaluation of three controller configurations' efficacy using control variability grid analysis. The SC–SC design (white circles, A zone 4%, B zone 86%, C zone 4%, D zone 6%, and E zone 0%), the SC^{MFB}–SC design (gray triangles, A zone 42%, B zone 55%, C zone 1%, D zone 2%, and E zone 0%), and the IP–SC design (black × marks, A zone 17%, B zone 83%, C zone 0%, D zone 0%, and E zone 0%) cases are presented. Also, the average and standard deviation of the 100 subjects from SC–SC design (red circle and white ellipse), SC^{MFB}–SC design (red triangle and light blue ellipse), and IP–SC design (red × mark and black ellipse) are presented. The *X* and *Y* coordinates represent the minimum and maximum blood glucose concentration of a subject with 95% confidence level during the protocol, respectively. (For interpretation of the references to color in this figure legend, the reader is referred to the web version of the article.)

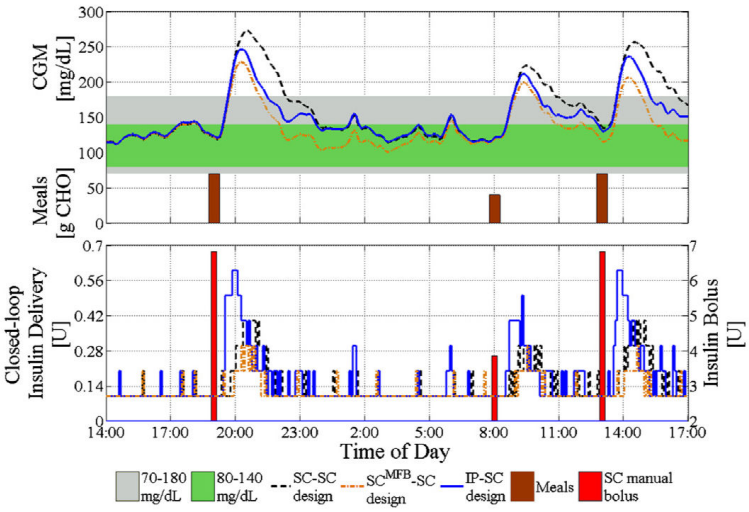

Fig. 9.

Representative example of control actions from three different configurations Top panel: Continuous glucose monitor traces of the SC–SC design (black dashed), the SC^{MFB}–SC design (orange dashed-dot), and the IP–SC design (blue solid) cases. Also, the meal sizes (black bars) are indicated, Bottom panel: Insulin delivered via an insulin pump in the SC–SC design (black dashed), the SC^{MFB}–SC design (orange dashed-dot), and the IP–SC design (blue solid). Also, the sizes of SC manual boluses are indicated (red bars) on the right *y*-axis. (For interpretation of the references to color in this figure legend, the reader is referred to the web version of the article.)

Table 1

Summary of artificial pancreas designs.

	Meal measurement and announcement (an anticipatory action to the meal by the user and controller's awareness of the action)	**Insulin delivery route**	**Glucose measurement route**
Closed-loop AP based on IP insulin delivery and SC CGM design (IP–SC)	No	IP	SC
Closed-loop AP based on SC insulin delivery and SC CGM design (SC–SC)	No	SC	SC
AP with manual feedforward SC bolus and SC CGM (SC^{MFB}–SC)	Yes	SC	SC

Table 2

Locations of the poles of the identified models for the ten subjects.

Subject	p_1	p_2	p_3
1	0.9870	0.7640 + 0.1721i	0.7640 − 0.1721i
2	0.9794	0.7839	0.5179
3	0.9863	0.7336 + 0.0512i	0.7336 − 0.0512i
4	0.9812	0.7218 + 0.2039i	0.7218 − 0.2039i
5	0.9840	0.7852	0.4233
6	0.9867	0.6823 + 0.0366i	0.6823 − 0.0366i
7	0.9824	0.7037 + 0.2097i	0.7037 − 0.2097i
8	0.9819	0.7328 + 0.1455i	0.7328 − 0.1455i
9	0.9813	0.7310 + 0.0205i	0.7310 − 0.0205i
10	0.9812	0.7440 + 0.0566i	0.7440 − 0.0566i

Table 3

Estimated closed-loop bandwidth and rise time of the ten systems (e.g., the combination of the controller and the subject 1 is called system 1).

System	Estimated closed-loop bandwidth [rad/min]	Rise time [min]
1	1.7×10^{-2}	120
2	1.4×10^{-2}	140
3	2.0×10^{-2}	100
4	4.9×10^{-2}	41
5	1.7×10^{-2}	120
6	2.7×10^{-2}	74
7	8.0×10^{-2}	25
8	1.4×10^{-2}	140
9	1.2×10^{-2}	160
10	1.2×10^{-2}	160

Table 4

Percent of time in the clinically accepted region (70–180 mg/dL) and the tight glucose range (80–140 mg/dL).

	Total (27 h)	4 h postprandial	Overnight (24:00–8:00)
70–180 mg/dL			
SC–SC design	83%[a]	67%[a]	96%
SC^{MFB}–SC design	97%	88%	99%
IP–SC design	96%[a]	87%[a]	99%
80–140 mg/dL			
SC–SC design	58%[a]	25%[a]	87%[a]
SC^{MFB}–SC design	79%[b]	45%[b]	94%
IP–SC design	69%[a,b]	32%[a,b]	94%[a]

[a] p-value < 0.01 for the paired t-test comparing the SC–SC design and the IP–SC design.

[b] p-value < 0.01 for the paired t-test comparing the SC^{MFB}–SC design and the IP–SC design.

Table 5

Average blood glucose risk indices of 100 in silico subjects.

	Low Blood Glucose Index	High Blood Glucose Index
SC–SC design	0.20	2.74[a]
SC^{MFB}–SC design	0.20	1.10[b]
IP–SC design	0.14	1.53[a,b]

[a] p-value < 0.01 for the paired t-test comparing the SC–SC design and the IP–SC design.

[b] p-value < 0.01 for the paired t-test comparing the SC^{MFB}–SC design and the IP–SC design.

Table 6

Percent of time in the clinically accepted region (70–180 mg/dL) and the tight glucose range (80–140 mg/dL). Zone-MPC for the IP–SC design was used in this evaluation.

	Total (27 h)	4 h postprandial	Overnight (24:00–8:00)
70–180 mg/dL			
50% Underestimated model gain	91%	89%	99%
Nominal model gain	96%	87%	99%
50% Overestimated model gain	87%	83%	99%
80–140 mg/dL			
50% Underestimated model gain	67%	36%	95%
Nominal model gain	69%	32%	94%
50% Overestimated model gain	63%	27%	94%

Table 7

Number of individuals who experienced hypoglycemia (BG < 70 mg/dL) and severe hypoglycemia (BG < 50 mg/dL). Zone-MPC for the IP–SC design was used in this evaluation.

	Number of individuals who experienced mild hypoglycemia (50 mg/dL < BG < 70 mg/dL)	Average low blood glucose index for the people who experienced hypoglycemia	Number of individuals who experienced severe hypoglycemia (BG < 50 mg/dL)
50% Underestimated model gain	4	0.42	0
Nominal model gain	3	0.35	0
50% Overestimated model gain	3	0.31	0